

Supplementary Material

Selective perfluorooctanoic acid (PFOA) and perfluorooctane sulfonate (PFOS) adsorption by nanoscale zero-valent iron (nZVI): Performance and mechanisms

Junhua Fang^a, Kairan Xu^b, Airong Liu^a, Yinghao, Xue^a, Luna Tie^a, Rongliang Qiu^{b, c},

Wei-xian Zhang^{a, c}, Zilong Deng^{a, *}

^a College of Environmental Science and Engineering, State Key Laboratory of Pollution Control and Resource Reuse, Tongji University, Shanghai 200092

^b South China Agricultural University, College of Natural Resources and Environment, Guangdong Provincial Key Laboratory of Agricultural & Rural Pollution Abatement and Environmental Safety, Guangzhou 510642

^c Guangdong Laboratory for Lingnan Modern Agriculture, Guangzhou 510642

*Corresponding author. Email: zilongdeng@tongji.edu.cn

Contents

Text S1. Adsorption kinetics.	3
Text S2. Adsorption isotherm.....	3
Text S3. Thermodynamic Calculations.	3
Text S4. The method of calculating adsorption energies.	4
Text S5. Electrochemical measurements.....	5
Table S1. Physical parameters of four iron-based materials.....	5
Table S2. Formula, molecular weight, octanol-water partition coefficient (K_{ow}), and acid dissociation constant (pK_a) of the PFOA and PFOS.....	5
Table S3. Kinetic parameters of the pseudo-first-order and pseudo-second-order equations for PFOA/PFOS adsorption on nZVI.	6
Table S4. Fitting parameters of intraparticle diffusion of PFOA and PFOS adsorbed by nZVI.	6
Table S5. Rate constants of Langmuir and Freundlich models for the adsorption of PFOS and PFOA on nZVI.....	6
Table S6. Fitted Langmuir isotherm parameters and thermodynamic calculations.....	7
Table S7. Binding energy data.	7
Figure S1. Simulated structures of (a) PFOA and (b) PFOS after geometry optimization. Carbon, oxygen, sulfur, hydrogen, and fluorine atoms are shown in gray, red, yellow, white, and cyan, respectively.	8
Figure S2. The EDS spectra and element composition (insert graph) of (a) nZVI, (b) PFOA-adsorbed nZVI, and (c) PFOS-adsorbed nZVI.	9
Figure S4. Adsorption energies of PFOA and PFOS on nZVI.	11
Figure S5. Electrochemical impedance spectroscopy of nZVI before and after adsorption of PFOA/PFOS.....	12

Text. S1. Adsorption kinetics.

Pseudo-first-order (S1), pseudo-second-order (S2), and intra-particle diffusion model (S3) are used to fit the adsorption process of PFOA/PFOS by nZVI, and the equation is as follows.

$$q_t = q_e \cdot (1 - e^{-k_1 \cdot t}) \quad (\text{S1})$$

$$q_t = \frac{k_2 \cdot q_e^2 \cdot t}{1 + k_2 \cdot q_e \cdot t} \quad (\text{S2})$$

$$q_t = k_p t^{1/2} + C \quad (\text{S3})$$

Where q_t and q_e represent the phosphate sorption capacity at a certain time and equilibrium, k_1 , k_2 , and k_p are the rate constants of pseudo-first-order model, pseudo-second-order model, intra-particle diffusion model, respectively.

Text. S2. Adsorption isotherm.

Langmuir and Freundlich adsorption isotherm models were used to describe the adsorption of PFOA and PFOS in materials. The nonlinear equations for the Langmuir (S4) and Freundlich (S5) models are shown as follows:

$$\frac{C_e}{q_e} = \frac{C_e}{q_m} + \frac{1}{q_m K_L} \quad (\text{S4})$$

$$\ln q_e = \frac{1}{n} \ln C_e + \ln K_F \quad (\text{S5})$$

Here, q_e (mg g^{-1}), q_m (mg g^{-1}), and C_e (mg L^{-1}) stand for the equilibrium sorption capacity, the maximum sorption capacity, and PFOA/PFOS concentration at equilibrium. K_L (L mmol^{-1}) is the Langmuir constant. K_F (mg g^{-1}) and $1/n$ represent Freundlich's sorption capacity and heterogeneity factor, a parameter for adsorption intensity and surface heterogeneity. The favorable range of $1/n$ is between 0 and 1.

Text S3. Thermodynamic Calculations.

Thermodynamic parameters for PFAS adsorption were first estimated using the Gibbs free energy equation and the linearized van't Hoff equation (i.e., the van't Hoff plot) as follows:

$$\Delta G^0 = -RT \ln K \quad (\text{S6})$$

$$\ln K = -\frac{\Delta H^0}{RT} + \frac{\Delta S^0}{R} \quad (\text{S7})$$

where ΔG^0 (kJ mol⁻¹) is the change of free energy, ΔH^0 (kJ mol⁻¹) is the change of enthalpy, ΔS^0 (kJ mol⁻¹) is the change of entropy, T (K) is the absolute temperature, R is the ideal gas constant (0.008314 kJ mol⁻¹ K⁻¹), and K is the dimensionless equilibrium coefficient. K can be estimated from the Langmuir constant (K_L) as:

$$K = K_L * C_w \quad (\text{S8})$$

where C_w is the water concentration (5.56×10^4 mmol L⁻¹).

Because adsorption enthalpy changes with surface coverage of adsorbed PFAS, assessing the enthalpy changes with increasing PFAS adsorption (q_e) would be useful to understand the interaction between PFAS and nZVI. Thus, the observed molar differential enthalpies (ΔH_{obs}) of PFAS adsorption on nZVI were further estimated using the differential van't Hoff equation:

$$\Delta H_{obs} = -R \frac{d(\ln(\frac{q_e}{C_e}))}{d(\frac{1}{T})} \quad (\text{S9})$$

At any given q_e , C_e was computed using the Langmuir parameters obtained at different temperatures. ΔH_{obs} was then calculated from the slope of the linear plots of $\ln(q_e/C_e)$ versus $1/T$.

Text S4. The method of calculating adsorption energies.

The adsorption energy (E_{ad}) can be calculated by the following expression:

$$E_{ad} = E_{surf+ad} - E_{surf} - E_{gas}$$

where $E_{\text{surf+ad}}$, E_{surf} and E_{gas} refer to the energy of PFOA/PFOS adsorbed on the surface, the energy of bare surface and the gas energy of PFOA/PFOS.

Text S5. Electrochemical measurements

Electrochemical impedance spectroscopy (EIS) was used to determine R_{CT} (charge transfer resistance), and EIS was performed at frequencies ranging from 0.1 MHz to 0.01 Hz at open circuit potential with a potential amplitude of 50 mV. The chronoamperometry is carried out at open circuit voltage. Tafel scans were performed by polarizing work electrodes ± 500 mV with respect to the open circuit potential at a scan rate of 10 mV s⁻¹. The corrosion currents I_{corr} was estimated from the Tafel plots by using both cathodic and anodic branches of the potentiodynamic polarization curves.

Table S1. Physical parameters of four iron-based materials

Adsorbent	Average size (nm)	specific surface area (m ² /g)
nZVI	60	25–35
FeOOH	50	76
Fe ₂ O ₃	30	90
Fe ₃ O ₄	30	66

Table S2. Formula, molecular weight, octanol-water partition coefficient (K_{ow}), and acid dissociation constant (pKa) of the PFOA and PFOS.

	Formula	Molecular weight, g/mol	Log K_{ow}^a , log (L/L)	pKa
PFOA	C7F15COOH	414.07	4.30	-0.2 ¹
PFOS	C8F17SO3K	538.22	5.25	-3.27 ²

Table S3. Kinetic parameters of the pseudo-first-order and pseudo-second-order equations for PFOA/PFOS adsorption on nZVI.

Adsorbent	Pseudo-first-order parameter			Pseudo-second-order parameter		
	q_e (mg/g)	k_1 (h ⁻¹)	R^2	q_e (mg/g)	v_0 (mg/g/h)	R^2
PFOA	5.208	0.808	0.942	5.527	3.394	0.967
PFOS	133.816	0.411	0.968	141.044	56.338	0.995

Table S4. Fitting parameters of intraparticle diffusion of PFOA and PFOS adsorbed by nZVI.

Adsorbent	Stage 1			Stage 2			Stage 3		
	K_{d1}	C_1	R_1^2	K_{d2}	C_2	R_2^2	K_{d3}	C_3	R_3^2
PFOA	1.61	0.94	0.99	0.57	2.93	0.99	0.03	5.20	0.96
PFOS	32.76	14.56	0.99	19.51	42.48	0.99	-0.04	134.27	0.25

Table S5. Rate constants of Langmuir and Freundlich models for the adsorption of PFOS and PFOA on nZVI.

Adsorbent	Langmuir parameters			Freundlich parameters		
	q_m (mg/g)	K_L (L/mg)	R^2	K_f (mg/g)	n	R^2
PFOA	17.632	0.185	0.985	3.734	2.137	0.975
PFOS	256.239	0.296	0.957	96.808	3.374	0.941

Table S6. Fitted Langmuir isotherm parameters and thermodynamic calculations.

Adsorbent	Temperature (K)	Langmuir parameters			thermodynamics		
		q_m (mg/g)	K_L (L/mg)	R^2	ΔG° (kJ mol ⁻¹)	ΔH° (kJ mol ⁻¹)	ΔS° (kJ mol ⁻¹ K ⁻¹)
PFOA	298	17.632	0.185	0.985	-37.818		
	308	12.301	0.155	0.988	-38.634	-13.894	0.080
	318	6.155	0.130	0.990	-39.424		
PFOS	298	256.239	0.296	0.941	-39.450		
	308	181.441	0.053	0.992	-36.37	-90.639	-0.1732
	318	90.573	0.03	0.987	-36.046		

Table S7. Binding energy data.

Substance	Binding energy (eV)	The types of bonds	Atomic %
nZVI	284.76	C–C	73.88
	286.41	C–OH	11.26
	288.55	C=O	14.86
nZVI	284.76	C–C	67.39

Substance	Binding energy (eV)	The types of bonds	Atomic %
nZVI	284.76	C–C	73.88
	286.41	C–OH	11.26
	288.55	C=O	14.86
+PFOA	286.38	C–OH	9.9
	288.82	C=O	14.71
	291.53	CF ₂	6.47
	294.31	CF ₃	1.53
nZVI +PFOS	284.84	C–C	49.47
	286.39	C–OH	8.4
	289.13	C=O	14.46
	291.77	CF ₂	21.19
	294.1	CF ₃	6.48

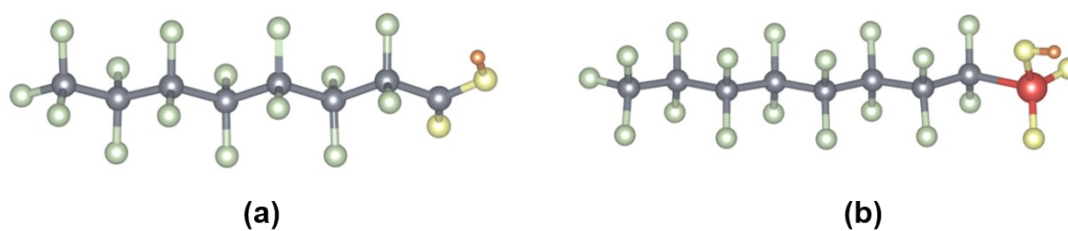


Figure S1. Simulated structures of (a) PFOA and (b) PFOS after geometry optimization. Carbon, oxygen, sulfur, hydrogen, and fluorine atoms are shown in gray, red, yellow, white, and cyan, respectively.

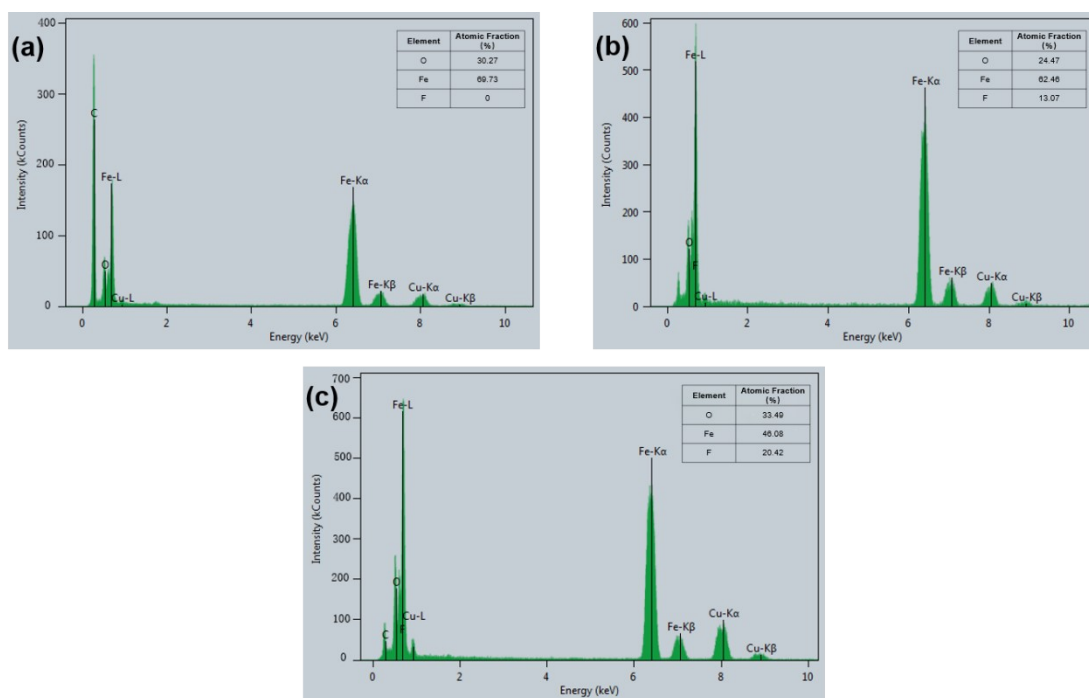


Figure S2. The EDS spectra and element composition (insert graph) of (a) nZVI, (b) PFOA-adsorbed nZVI, and (c) PFOS-adsorbed nZVI.

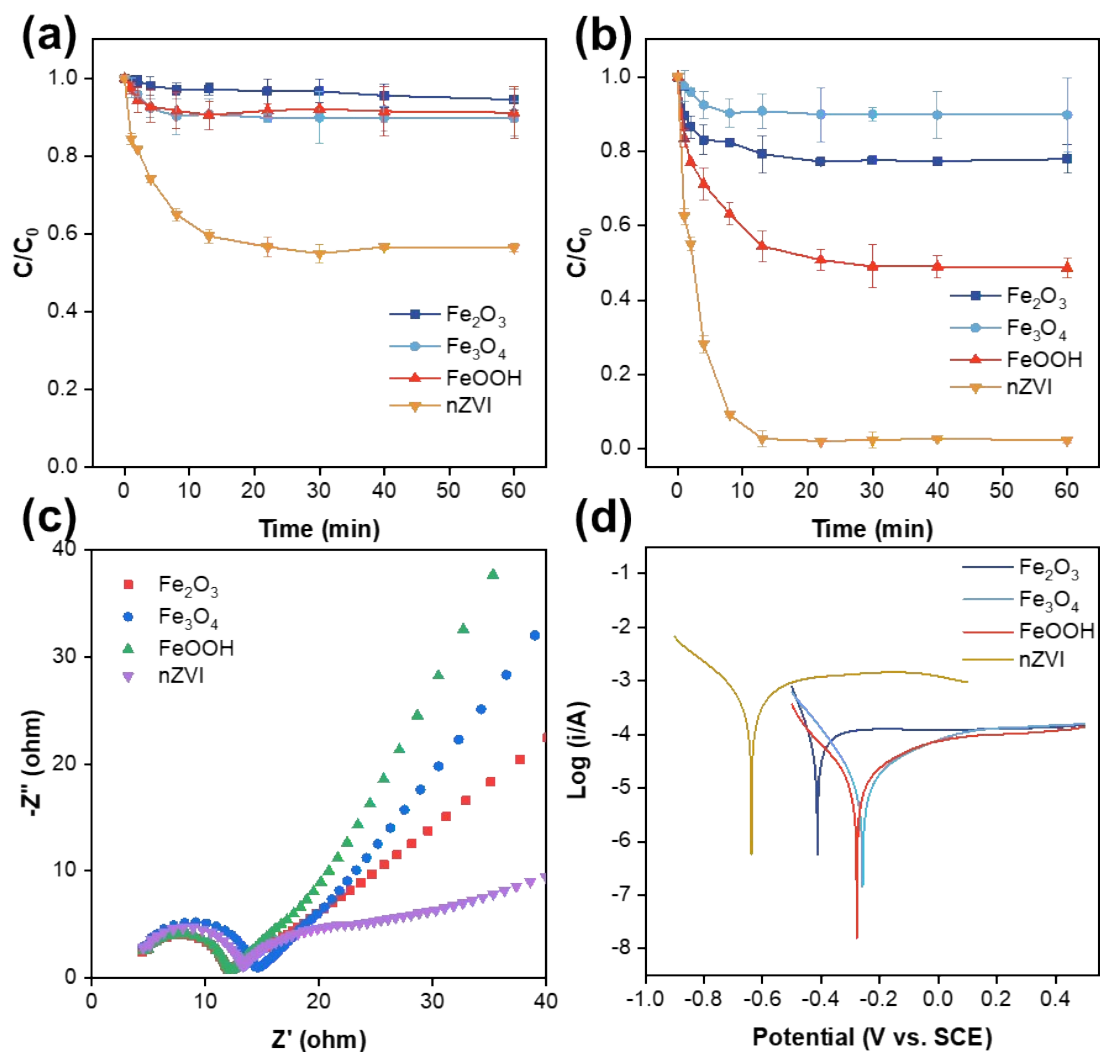


Figure S3. Removal of PFOA (a) and PFOS (b) by different iron-based materials. Experimental conditions: 1 mg/L PFOA / 10 mg/L PFOS, 0.2 g/L iron-based materials (Fe_2O_3 , Fe_3O_4 , $FeOOH$, nZVI), and initial pH 7.0. (c) Electrochemical impedance spectra (d) Tafel profiles of Fe_2O_3 , Fe_3O_4 , $FeOOH$, and nZVI.

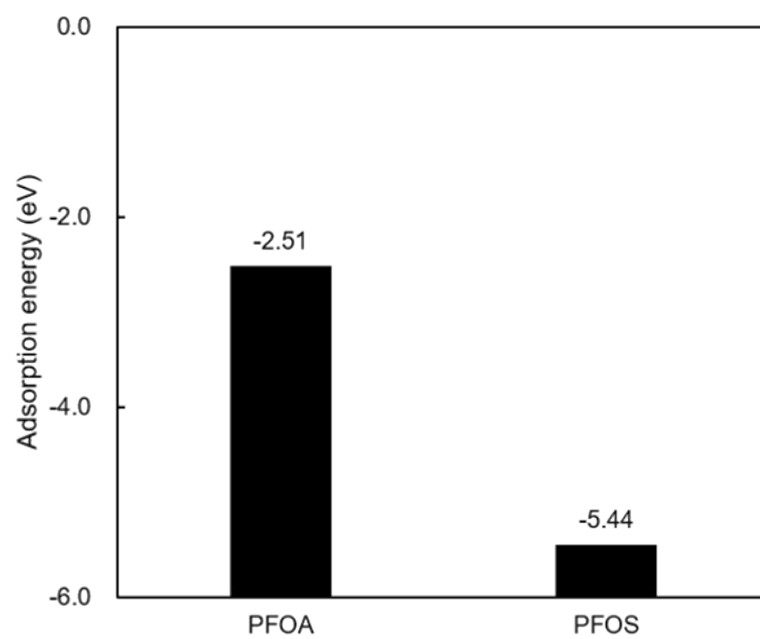


Figure S4. Adsorption energies of PFOA and PFOS on nZVI.

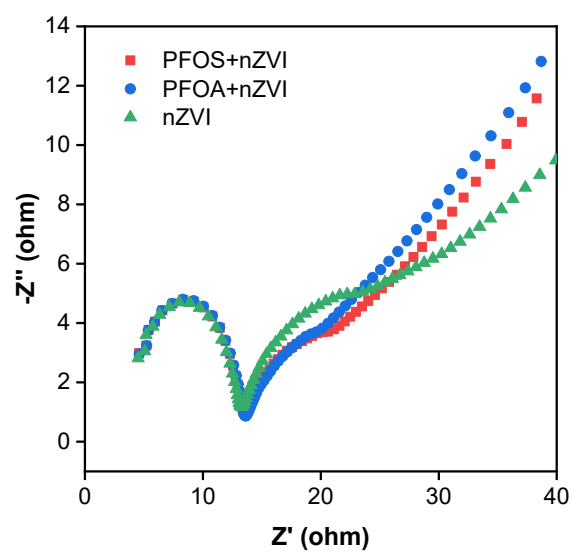


Figure S5. Electrochemical impedance spectroscopy of nZVI before and after adsorption of PFOA/PFOS.

References

1. S. Rayne and K. Forest, Theoretical studies on the pKa values of perfluoroalkyl carboxylic acids, *Journal of Molecular Structure-Theochem*, 2010, **949**, 60-69.
2. Y. Zhang, Y. Zhi, J. Liu and S. Ghoshal, Sorption of Perfluoroalkyl Acids to Fresh and Aged Nanoscale Zerovalent Iron Particles, *Environmental Science & Technology*, 2018, **52**, 6300-6308.